Hindawi
Advances in Civil Engineering
Volume 2019, Article ID 5409013, 16 pages
https://doi.org/10.1155/2019/5409013

Research Article

Extending the Fatigue Life of Steel Truss Bridges with Tuned Mass Damper Systems

Alessio Pipinato

Department of Structural Engineering, AP&P Institute, Rovigo 45100, Italy

Correspondence should be addressed to Alessio Pipinato; alessio.pipinato@gmail.com

Received 3 January 2019; Accepted 20 March 2019; Published 14 April 2019

Academic Editor: Stefano Sorace

The increasing traffic demand is continuously growing worldwide. Therefore, the life of a large stock of bridges that still exist throughout the world must be extended, ensuring at the same time that safety is not compromised for economic reason. This paper introduces the possibility to control the fatigue life of existing bridges by using a vibration control system. Based on a dynamic optimization analysis, the stresses from traffic on the bridge are obtained. Subsequently, a plate finite element (FE) model of the whole bridge is developed. The equation of motion is presented for a case study bridge, equipped with different tuned mass damper system, and the combination of external loads and train/track interaction with or without the TMD system is developed through own-developed routines and FEM software. The procedure is showcased for a case study bridge. After gaining the stress states at the critical hotspot, the fatigue crack life is evaluated by using the linear cumulative damage theory. The different TMD solution presented is demonstrated to be able to diminish the stress level in critical hotspots, improving the overall fatigue life of the bridge over an established lifetime.

1. Introduction

Fatigue failure of steel bridges is a well-known event that is frequently reported across the world [1–3]. As a fact, bridges are a strategic part of an ancient transport network and, in some cases, they are at the limits of the traffic capacity. In the particular case of steel bridges, truss bridges were widely used during road construction from the second half of the 19th century up to the middle of the 20th century. Most of these wrought iron or older steel bridges, which are still in use around Europe, were not designed explicitly for continuously increasing vehicle numbers and weight. ASCE [1] reported that 80–90% of failures in steel structures are related to fatigue and fracture. However, other factors affecting the structural aging of bridges are reported in [4–15]. Vibrations, transverse horizontal forces, internal constraints, and localized and diffused defects as corrosion damages are concurring causes of damages [16]. The main problems recognized by the managing agencies are related to difficulties in maintenance, high noise emissions and vibrations, fatigue, and understrength capacities mainly found in transverse, main girders, and their riveted or bolted connections, while the main load-bearing elements (trusses) still have some residual capacity [17]. Another major problem is the inability to carry the actual Eurocode live loads [18]. It should be noticed that rarely a load reduction is approved for road of national importance (highway and national road, railways); and for this reason, existing bridges must carry the traffic category requested for new bridges [18]. Actually, a total replacement of these bridges is not possible due to financial constraints. Moreover, most of these bridges have not yet fulfilled their design life, and in some cases, their main structures are in a good condition, except specific understrength members. However, it should be mentioned that no design life was ever defined for the large majority of existing bridges, which means that implicitly they are supposed to last as long as the utilization (e.g., for road traffic) is given. For this reason, it is crucial to implement solutions to strengthen bridges, or to control peak stresses in order to avoid fatigue failures. While retrofit solutions have been broadly investigated in the literature [17, 19, 20], a few of the literature studies investigate fatigue control in bridges by using TMD systems. These can extend the life of existing steel bridges, similar to the common use for the control of vibration. The TMD has proved to be very effective for providing the harmonic force acting at a fixed location on the beam structure [21–36], and it might be effective as well for a moving load [37]. Using the same approach of TMD, MTMDs (multiple TMD) systems have been proved to be effective for reducing the dynamic response of continuous truss bridges to moving train loads [38, 39]. It has been found that MTMDs are generally more effective and reliable than a single TMD for suppressing the resonant vibrations of bridges when the train axle arrangement is regular. MTMDs fundamentals could be found in [29]; and applications could be deepened in [40] for wind issues or [41] for train-induced vibration controls. Recent applications of MTMDs investigated also combined external loads, as seismic and passing trains simultaneously (as in [42]).

2. Equation of Motion

The vibration absorber is a mechanical device used to decrease or eliminate unwanted vibration [43]. The denomination TMD-tuned mass damper is often used in modern installation; this modern name has the advantage of showing its relationship to other types of dampers. In its simplest form, a vibration absorber consists of one spring and a mass. Such an absorber system is attached to a SDF system. Tuned mass damper (TMD) is among the oldest types of vibration absorbers, invented by Frahm in 1909, according to the study in [24].

An Euler–Bernoulli beam with j spans (Figure 1) is introduced to explain the formulation of the equation of motion. The beam is subjected to a distributed load $p(x, t)$, on span i with length L_i. To avoid complexity in this phase, it is considered that the mass per unit length m, Young's modulus E, and moment of inertia I are constant within each span, varying at intermediate supports. An MTMD bridge system could be studied according to recent research [44–47] reported. To obtain equilibrium (reference to Figure 1), neglecting higher order terms, it should be

$$\uparrow: m(x)\frac{\partial^2 w(x,t)}{\partial t^2} + c(x)\frac{\partial w(x,t)}{\partial t} - \frac{\partial V}{\partial x} = p(x,t), \quad (1)$$

$$\begin{aligned}\circlearrowleft: V &+ \frac{\partial V}{\partial x}\partial x + \frac{\partial M}{\partial x} + p(x,t)\frac{\partial x}{2} - m(x)\frac{\partial^2 w(x,t)}{\partial t^2}\frac{\partial x}{2} \\ &- c(x)\frac{\partial w(x,t)}{\partial t}\frac{\partial x}{2},\end{aligned} \quad (2)$$

$$V = -\frac{\partial M}{\partial x}, \quad (3)$$

$$\frac{\partial M}{\partial x} = \frac{\partial}{\partial x}\left(E(x)I(x)\frac{\partial^2 w(x,t)}{\partial x^2}\right). \quad (4)$$

And substituting Equation (4) in Equation (3),

$$\begin{aligned} m(x)\frac{\partial^2 w(x,t)}{\partial t^2} &+ c(x)\frac{\partial w(x,t)}{\partial t} \\ &+ \frac{\partial^2}{\partial x^2}\left(E(x)I(x)\frac{\partial^2 w(x,t)}{\partial x^2}\right) = p(x,t).\end{aligned} \quad (5)$$

According to [43, 47], the transverse displacement $w(x, t)$ within a segment is obtained by solving Equation (5); to separate the general differential equation into a linear combination of normal modes $\phi_n(x)$, the expansion theorem is then used. Consider

$$w(x,t) = \sum_{n=1}^{\infty}\phi_n(x)q_n(t). \quad (6)$$

Given the coordinates of the n node, substituting into Equation (5), adopting the Dirac delta-function $\delta(p = P\delta(x - vt))$ to describe the concentrated moving load,

$$\begin{aligned}\sum_{n=1}^{\infty}\Bigg(& m(x)\frac{d^2 q_n(t)}{dt^2}\phi_n(x) + c(x)\frac{dq_n(t)}{dt}\phi_n(x) \\ &+ \frac{d^2}{dx^2}\left(E(x)I(x)\frac{d^2\phi_n(x)}{dx^2}\right)q_n(t)\Bigg) = P\delta(x - vt),\end{aligned} \quad (7)$$

where t is the time of the P concentrated moving load onto the i-span, at the v speed; it is suggested to apply undamped and free vibration conditions to Equation (5) to obtain an ODE (ordinary differential equation):

$$\frac{d^2}{dx^2}\left(E(x)I(x)\frac{d^2\phi_n(x)}{dx^2}\right) = m(x)\omega_n^2\phi_n(x). \quad (8)$$

Then combining Equations (8) and (7), we get

$$\begin{aligned}\sum_{n=1}^{\infty}\Bigg(&\frac{d^2 q_n(t)}{dt^2}m(x)\phi_n(x) + c(x)\frac{dq_n(t)}{dt}\phi_n(x) \\ &+ m(x)\omega_n^2\phi_n(x)q_n(t)\Bigg) = P\delta(x - vt).\end{aligned} \quad (9)$$

Furthermore, introducing $\phi_r(x)$ and integrating it gives

$$\begin{aligned}\sum_{n=1}^{\infty}\Bigg(&\frac{d^2 q_n(t)}{dt^2}\int_0^L m(x)\phi_n(x)\phi_r(x)dx \\ &+ \frac{dq_n(t)}{dt}\int_0^L c(x)\phi_n(x)\phi_r(x)dx \\ &+ \omega_n^2 q_n(t)\int_0^L m(x)\phi_n(x)\phi_r(x)dx\Bigg) \\ &= \int_0^L P\delta(x - vt)\phi_r(x)dx.\end{aligned} \quad (10)$$

And this reduces to

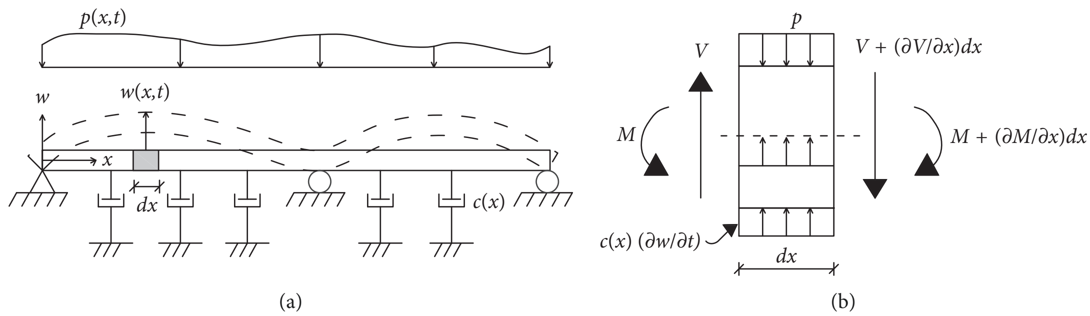

Figure 1: TMD system on a generic bridge structure (a). Infinitesimal segment of the body (b).

$$\frac{d^2 q_n(t)}{dt^2}\int_0^L m(x)\phi_n^2(x)dx + \frac{dq_n(t)}{dt}\int_0^L c(x)\phi_n^2(x)dx$$
$$+\,\omega_n^2 q_n(t)\int_0^L m(x)\phi_n^2(x)dx\int_0^L P\delta(x-vt)\phi_n(x)dx. \tag{11}$$

By the use of c_n (modal damping of the system), which is related to the modal damping ratio χ_n,

$$c_n = \int_0^L c(x)\phi_n^2(x)dx = 2\omega_n\zeta_n\int_0^L m(x)\phi_n^2(x)dx, \tag{12}$$

where $\omega_n = 2\pi f_n$ is the angular natural frequency of vibration (of the n mode), and substituting Equation (12) into Equation (11), the following is obtained:

$$\frac{d^2 q_n(t)}{dt^2}\int_0^L m(x)\phi_n^2(x)dx + 2\omega_n\zeta_n\frac{dq_n(t)}{dt}\int_0^L m(x)\phi_n^2(x)dx$$
$$+\,\omega_n^2 q_n(t)\int_0^L m(x)\phi_n^2(x)dx = \int_0^L P\delta(x-vt)\phi_n(x)dx. \tag{13}$$

Given the Dirac delta function, the following is used:

$$\int_{-\infty}^{\infty}\delta(x-vt)f(x)dx = f(vt), \tag{14}$$

and considering that the normal modes are mass-normalized, Equation (13) can finally be simplified to

$$\frac{d^2 q_n(t)}{dt^2} + 2\omega_n\zeta_n\frac{dq_n(t)}{dt} + \omega_n^2 q_n(t) = P\phi_n(x_v), \qquad n = 1,\ldots,\infty, \tag{15}$$

denoting with x_v the concentrate load P-position at t-time.

3. Train-Structure Interaction

The simplest interaction was studied by Saller [48]; in this formulation, the train-bridge moving load model is adopted, where the equation of motion is given by

$$m\frac{\partial^2 w}{\partial t^2} + c\frac{\partial w}{\partial t} + \frac{\partial^2}{\partial x^2}\left(EI\frac{\partial^2 w}{\partial x^2}\right) = \delta(x-vt)\left[P - m_v\frac{\partial^2 w}{\partial t^2}\right]. \tag{16}$$

However, FEM solution includes all the possibility to encompass in the train model interaction also the suspension of each axle, wheels unsprung mass, bogie axle, coach, and their mutual interaction (Figure 2).

However, some authors reported that a complex model of the bridge/train interaction is often negligible and that a moving load sufficiently describes the structural behavior of the bridge under a passing train. Examining different interaction analyses (multistatic or dynamic) and different train models with varying interaction systems, Liu et al. [49] found that the results are very similar if the natural frequency of the train (f_v) is much smaller than the natural frequency of the bridge (f_n), the mass of the train is smaller than the mass of the bridge, and the train is not moving at the critical speed. This should also be considered for the purpose of this study, which Eurocode [50] also suggests neglecting train/structure interaction (par. 6.4.6.4).

4. Soil-Structure Interaction

A similar conclusion could be achieved for the soil-structure interaction issue, which was analyzed extensively in [51–55]. All these studies confirmed that under approximately 150 km/h, soil-structure interaction could be disregarded. However, for high-speed train ($v > 200$ km/h), this issue becomes relevant and should be deepened. In order to cover this issue, FEM models should be easily designed with frequent dependent spring at the interface of structure foundation/soil. In the specific case, the railway line has an imposed speed limit of 150 km/h; consequently, soil-structure interaction issues have not been considered.

5. Damping Ratios

Although a refined solution includes the definition of bending of materials, opening and closing of cracks, friction at supports and bearings, ballast, train-structure interaction, and soil-structure interaction [56, 57], empirical and comprehensive ratios are used in structural engineering, derived from direct measurement on real bridges. An alternative computational method to model the energy dissipation deals with the introduction of distributed viscous dampers, which should be calibrated [43]. According to Eurocode [50], the values of damping reported in Table 1 should be used in the dynamic analysis.

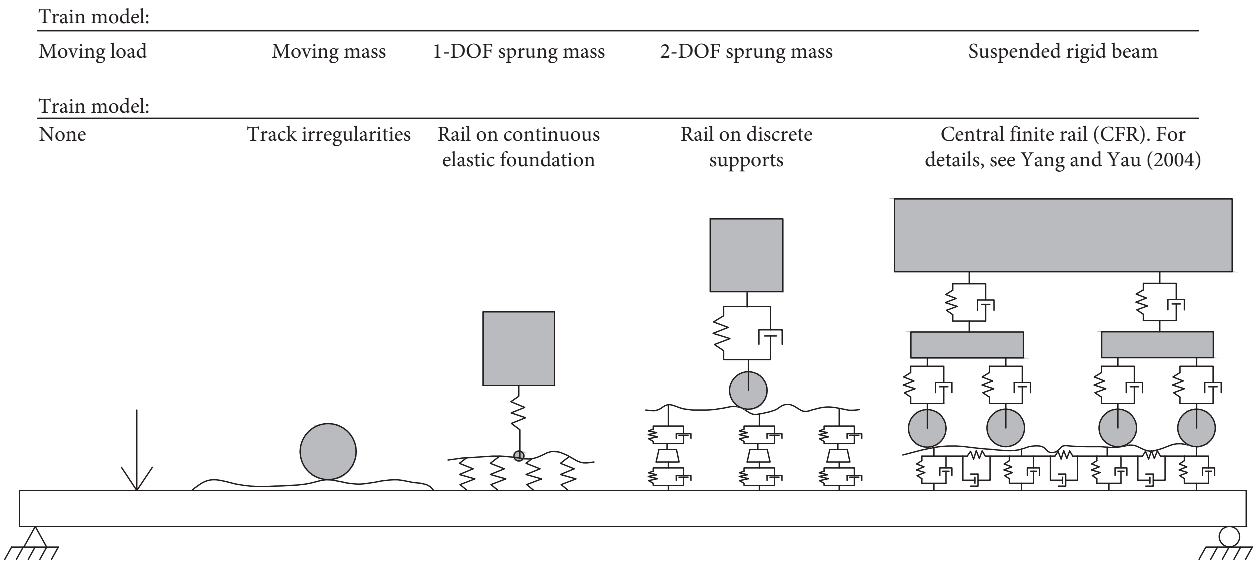

Figure 2: Train-track bridge model.

Table 1: Values of damping to be assumed for design purposes.

Bridge type	Lower limit of percentage of critical damping, ζ (%)	
	Span $L < 20$ m	Span $L \geq 20$ m
Steel and composite	$\zeta = 0.5 + 0.125$ (20-L)	$\zeta = 0.5$
Prestressed concrete	$\zeta = 1.0 + 0.07$ (20-L)	$\zeta = 1.0$
Filler beam and reinforced concrete	$\zeta = 1.5 + 0.07$ (20-L)	$\zeta = 1.5$

Moreover, Eurocode [50] suggests performing a dynamic analysis only at specific conditions.

6. Case study

This investigated case study is a 161 m through three spans (50.16 m–60.648 m–50.160 m ≈ 161 m) truss metal riveted railway bridge, 5.06 m wide (from the centre of mass of the lower chords) and 7.2 m high (from lower chord to the upper one) [58]. These spans are simply supported on the shoulders and on piles in the riverbed. The historical bridge was built in 1866, and after 40 years, the second parallel track was realized: these bridges were both destroyed during the II World War. The configuration of the bridge structure is presented in Figure 3: the even track was built in 1946 and the other one in 1949. The bridge studied is the oldest in service (from 1946). The actual configuration is presented in Figures 3–5. The superstructure consists of 32 different cross sections. Lower and upper chords are composed by U-shaped sections. The deck is composed by longitudinal stringers, and transverse floor beams, which have a fixed distance of 5.054 m, while stringers are at 1.520 m one to each other. All structural elements are built-up riveted members, realized with plates and L-profiles with variable width from 12 to 20 mm. Also, connection joints are made of gusset riveted plates. Rails are of the 60-UNI type. Boundary conditions are reported in Figure 3(c), double fixed and movable bearings stand alternately on each side span as shown. According to modern standards [59], the basic material can be compared to an S275 steel [18]. The FEM model of the bridge is reported in Figure 6. The bridge structure was modelled using the FEM software MIDAS Civil, using beam and plate elements. Overall, the entire bridge model consists of about 3000 beam and 200 plate elements. Young's modulus of 221 GPa (kN/mm^2), Poisson's ratio of 0.3, and a material density value of 7800 kg/m^3 were used for the analyses. All beam member sections were modelled as the as-built structure. One alternative model has been realized to take into account material degradation (e.g., reducing transversal section). The FEM model has been calibrated by in situ measurement [58].

The bridge modelled is subjected to the Instruction 44/F moving loads that represents the train (Table 2).

7. TMD Governing Equations and Optimization Routine

The FEM model results are compared to the numerical solution, where the bridge is modelled as a simply supported elastic beam with a constant cross section. The structure is subject to a series of moving loads with constant speed representing the train. Three different TMD devices are introduced: single TMD, multiple TMD (MTMD), and series of multiple tuned mass dampers (STMD), placed on the beam at $x = x_s$ as shown in Figure 7. Equations of the vertical motion for the bridge are derived and can be written as

$$EI \frac{\partial^4 w}{\partial x^4} + c_b \frac{\partial w}{\partial t} + m_b \frac{\partial^2 w}{\partial t^2} = F^{\text{train}} + F^{\text{tmd}}. \quad (17)$$

Upon solution of each equation for each type of mass damper (TMD, MTMP, and STMD) by direct methods [60],

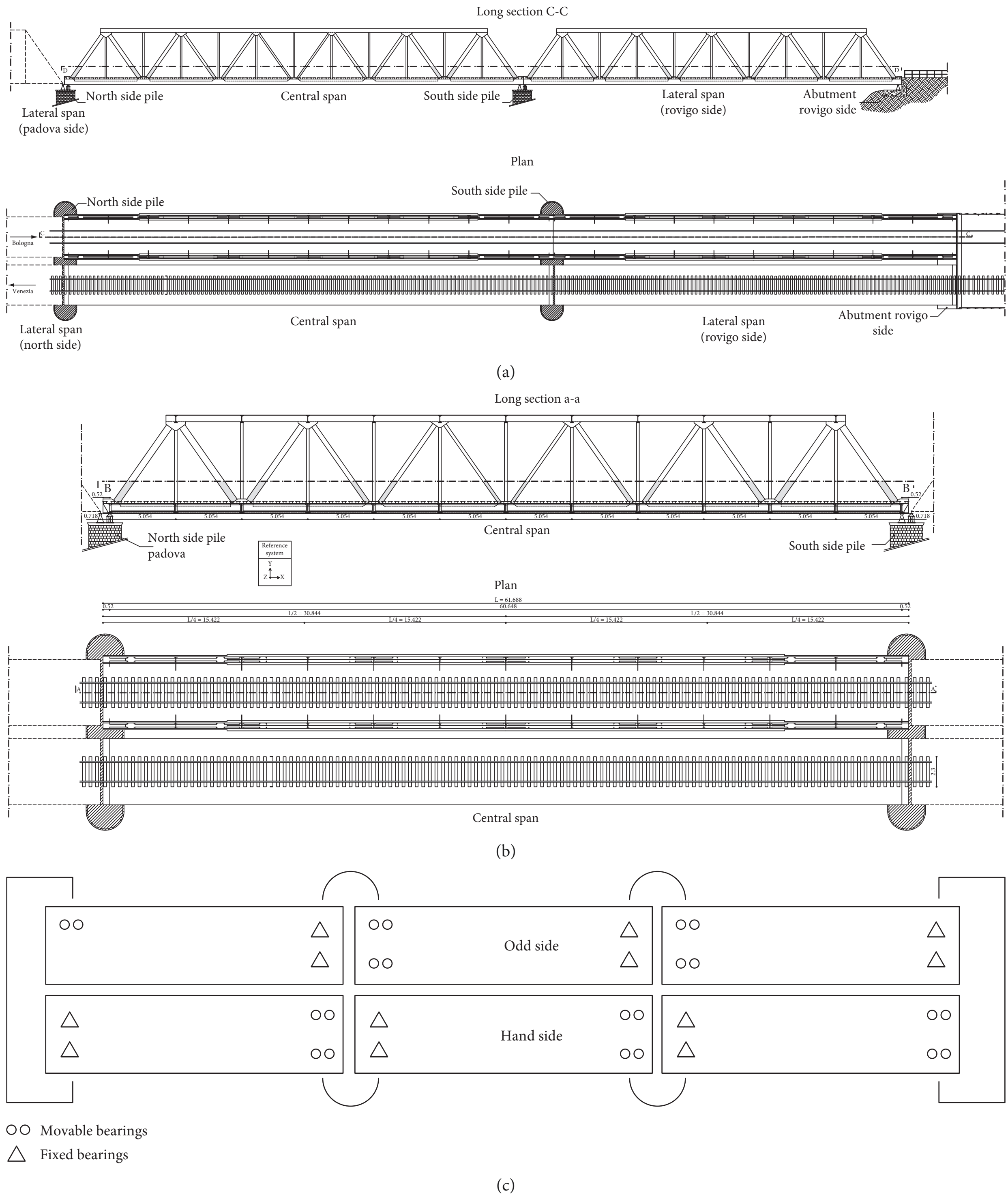

Figure 3: Case study: bridge: plan and long section of the central and south span (a); long section and plan of the central span (b); boundary conditions (c).

the equations of motion for the entire bridge-TMD system under a moving train can simply be expressed in the matrix form as follows:

$$M\ddot{u} + C\dot{u} + Ku = F, \quad (18)$$

where the mass (M), damping (C), and stiffness (K) matrices; the load vector F, and the unknowns vector u are given in [60]. Equation (20) can be solved numerically by Newmark's method to obtain unknown parameters.

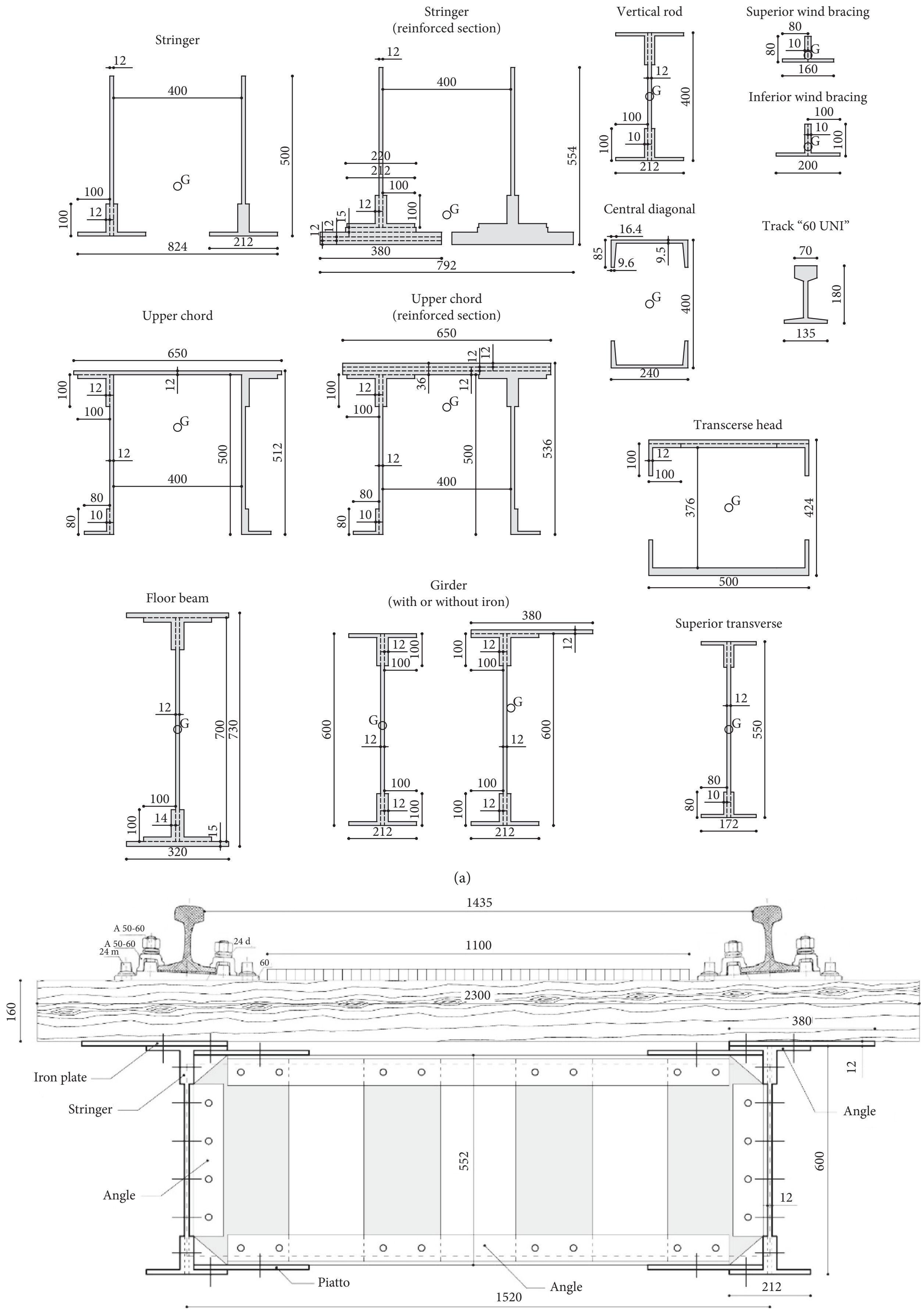

Figure 4: Case study: bridge (a) and built-up member details (b).

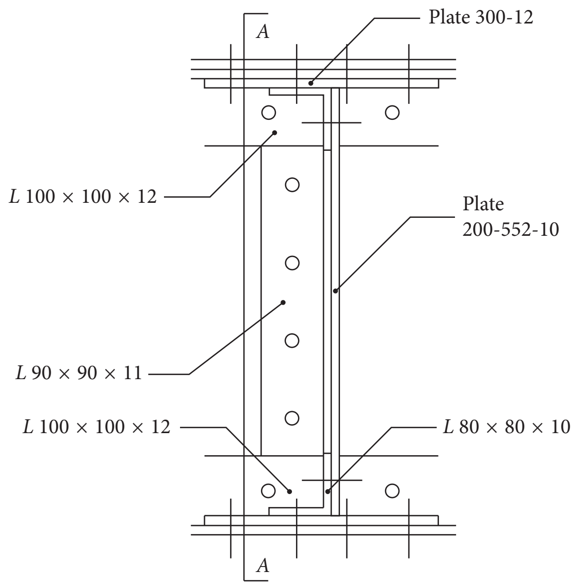

FIGURE 5: Riveted connection of transverse-to-stringer.

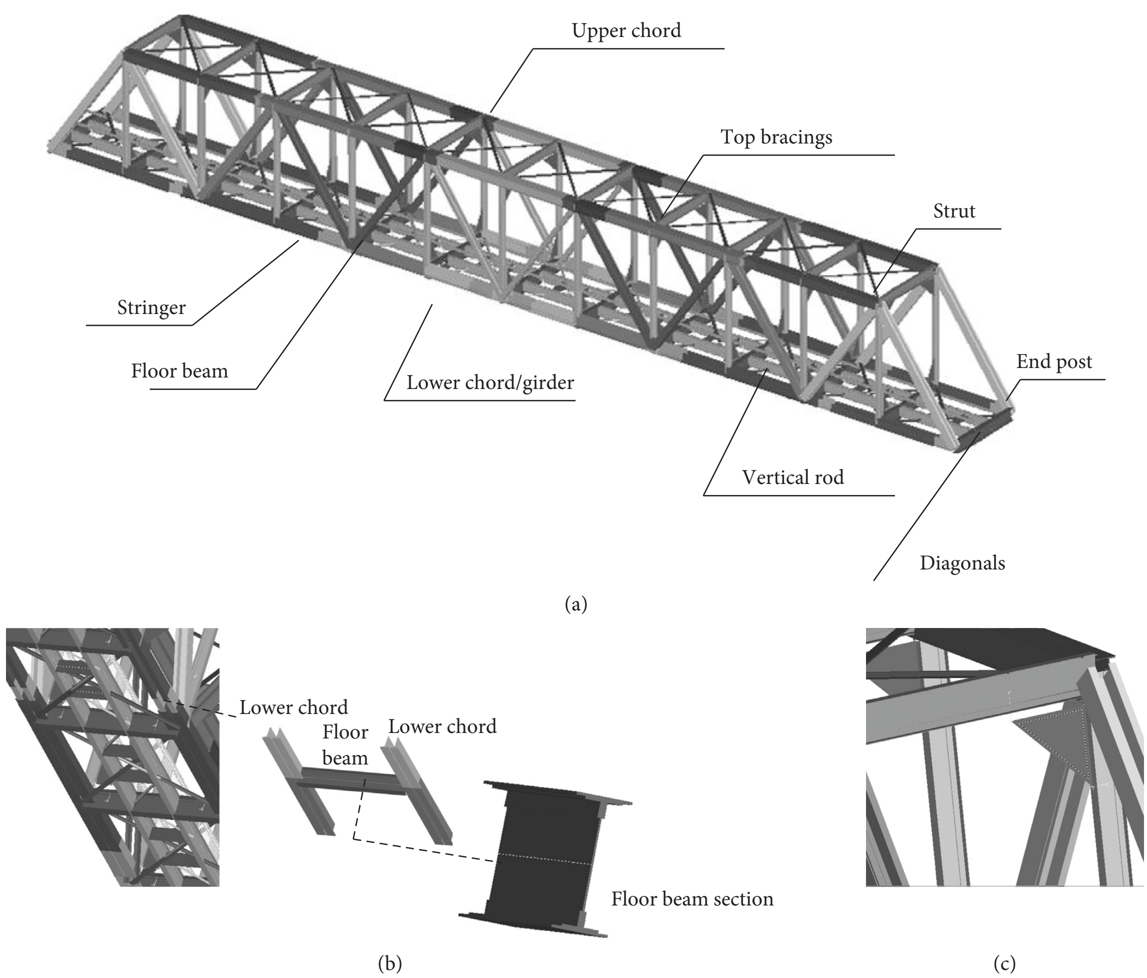

FIGURE 6: Case study: bridge: FEM model of the central span (a); details of the floor beams and lower chord (b); gusset plate of the cross-truss-portal (c).

Table 2: Instruction 44/F (1992): daily traffic spectrum and train loads for fatigue verification.

Train type	Name	Train/day	Axle/day	Locomotive (L) and carriages (Ci)	T/axle	Wagon number	Wagon type	Axle spacing (m)
1	IC	20	960	L	20,25	1	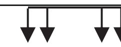	2.6–6.4–2.6
	Intercity			C1	15	5		2.56–16.44–2.56
				C2	12,75	6		2.56–16.44–2.56
2	EC	10	340	L	20	1	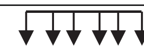	2.85–2.35–2.85–2.35–2.85
	Eurocity			C1	14,25	2		2.56–16.44–2.56
				C2	12	5		2.56–16.44–2.56
3	EXPR	15	990	L	20	1	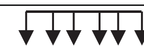	2.85–2.35–2.85–2.35–2.85
	Express			C1	14,25	10		2.56–16.44–2.56
				C2	12	5		2.56–16.44–2.56
4	DIR	30	1380	L	18,6	1	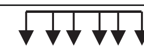	2.85–2.35–2.85–2.35–2.85
	Direct			C1	10,675	10		2.4–16.6–2.4
5	ETR	10	480	L	20	2	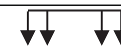	3–9–3
	Eurostar			C1	11,6	10	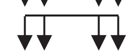	3–17.3–3
6	TEC	15	990	L	18,7	1	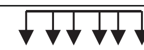	2.85–2.35–2.85–2.35–2.85
	Container freigh			C1	20	15	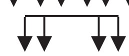	1.8–12.8–1.8
7	Merci acciaio	10	720	L	18,7	2	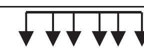	2.85–2.35–2.85–2.35–2.85
	Steel freight			C1	20	15	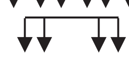	1.8–13.06–1.8
8	Treno merci tipo D4	5	380	L	20	2	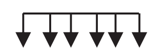	2.85–2.35–2.85–2.35–2.85
	D4 freight			C1	22,5	16	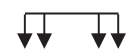	1.8–4.65–1.8
9	Treno merci misto	5	270	L	18,7	1	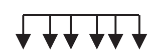	2.85–2.35–2.85–2.35–2.85
	Mixed freight			C1	16	24		9

The maximum stress oscillation found on the bridge according to the load case described in Table 2 has been presented in [58]: this has been found to be the stringer-to-floor beam connection, in detail at the lower flange of the floor beam where the stringer is jointed to the floor beam. Maximum stresses obtained by a multistatic and linear dynamic analysis are reported in Table 3 [58], considering also an FEM model with a corroded member: this model considered a cross-section reduction of 1 mm extended to the whole lower chords according to the similar case study described in [61].

Consequently, the optimization is obtained minimizing the maximum stress oscillation found on the bridge under the moving loads (Table 2) by adjusting the mass ratio $\mu = m_2/m_1$, the damping ratio ξ_j, and the frequency ratio $\beta_j = \omega_j/\overline{\omega}_1$ of STMD. The optimization problem is solved using a MATLAB nonlinear programming solver (*fmincon*) which finds the minimum of a constrained nonlinear multivariable function with the sequential quadratic programming (SQP) method. First, the start points and bounds are assigned for optimization of design parameters. Then, using the modal superposition method, the governing differential equations of the motion for the bridge-train TMD-coupled system are solved numerically. When the objective function is gained, the *fmincon* code is applied to update all parameters and checked if the objective function is minimum or not. When the objective function is minimized, the optimal parameters are obtained. According to this procedure, TMDs are introduced in the model, in order to simulate a real case study: TMD-1 ($\mu = 2\%$, concentrated at midspan), TMD-3 ($\mu_{1,2,3} = 0.9\%$, concentrated at the fourth of the span), TMD-7 ($\mu_{1,2...,7} = 0.4\%$, equally spaced onto the span length), and STMD ($\mu_1 = 0.8\%$, $\mu_2 = 0.9\%$, concentrated at midspan).

8. Results and Discussion

The procedure consists in finding the solution of the following:

$$\begin{gathered} \min J(p), \\ l_b < p < u_b, \end{gathered} \tag{19}$$

where $p = (\mu, \xi_j, \beta_j)$, $J(p)$, l_b and u_b represent the optimization variables, the objective function, the lower bound, the and

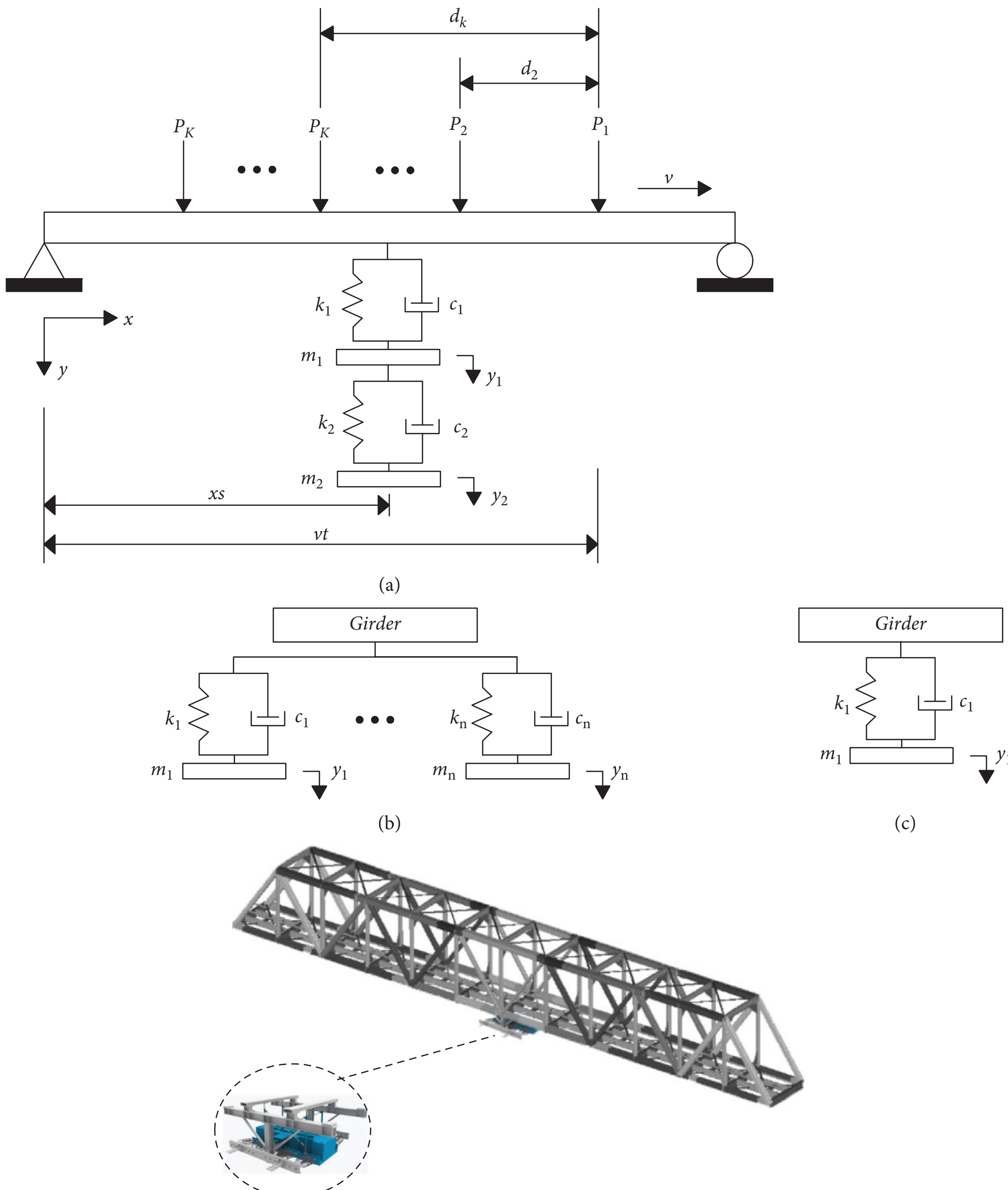

(d)

Figure 7: The simply supported beam representing the bridge subjected to moving train loads (a) series multiple TMD (STMD), (b) parallel multiple TMD (MTMD-n), and (c) classic TMD (TMD-1) [60]. Sketch example of TMD-1 installed on the bridge (d).

Table 3: Extreme values of the stresses in the structural members from the different models (Table 2). Results refer to train type 8.

Structural model	Stresses (MPa)					
	Stringer		Hanger plate		Floor beam	
	Max	Min	Max	Min	Max	Min
3D girder as-built	102	11	140	14	99	12
3D girder corroded	+1%	+1.2%	+1.3%	+1.1%	+1.2%	+1.3%

upper bound of the optimization variables, respectively. $J(p)$ is defined as maximum amplitude in frequency response of midspan. Assuming the damping ratio of the beam ξ_j and the total TMD mass to the beam mass ratio $\mu_{\mathrm{Tot}} = \Sigma\mu_j$ are known, we can select the following to be control parameters such as $0.0 < \mu < 1.0$, $0.8 < \beta_j < 1.2$, and $0.0 < \xi_j < 0.5$, according to the studies in [60, 62–64]. To optimize multiple TMDs in parallel, uniform stiffness and damping are assumed for all TMD units in the system according to the studies in [60, 65] since manufacturing of this type of absorbers is much simpler than those with varying stiffness and damping. To optimize MTMDs, the mass of each TMD unit varies according to the study in [66]. In all cases, the mass ratio μT is selected to be 2% according to the study in [60]. The consequent optimal parameters for TMD devices are obtained. In the analyses,

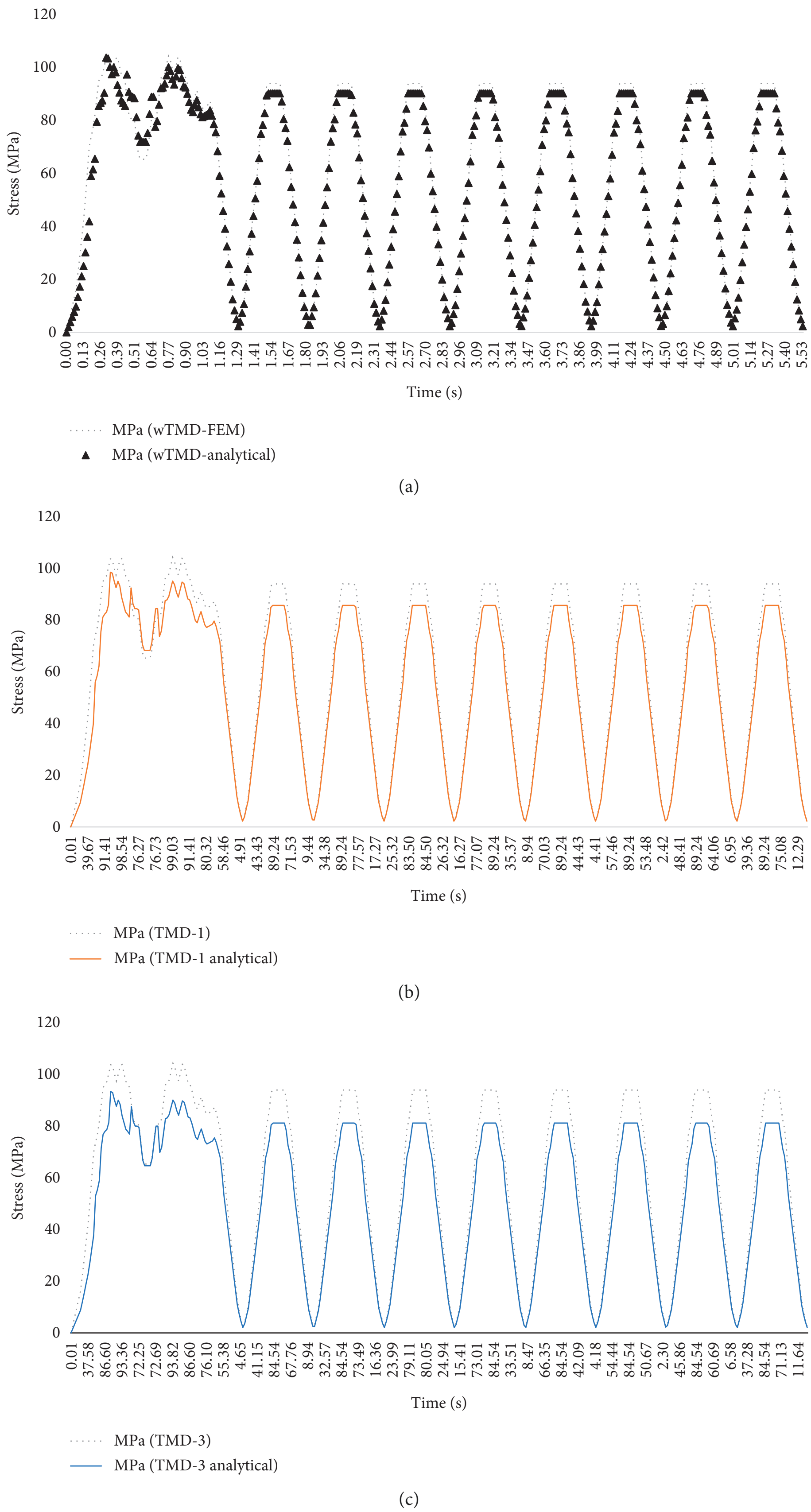

Figure 8: Comparison of the numerical and analytical dynamic analysis results for the hotspot detail: without intervention (a), with TMD-1 (b), and with TMD-3 (c).

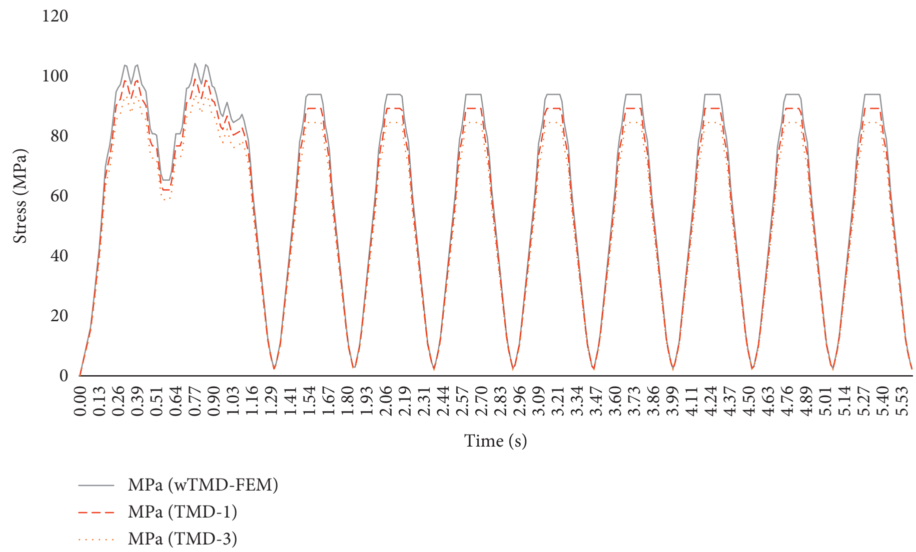

Figure 9: Comparison of the numerical dynamic analysis results for the hotspot detail: with (TMD-1, TMD-3) or without TMD solutions (wTMD-FEM).

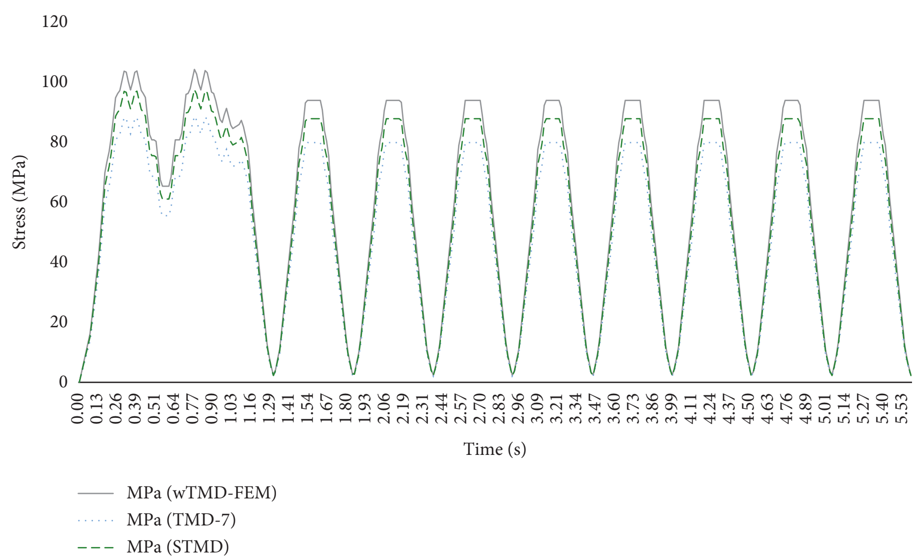

Figure 10: Comparison of the numerical dynamic analysis results for the hotspot detail: with (TMD-7, STMD) or without TMD solutions (wTMD-FEM).

different types of vibration absorbers such as a single TMD (TMD-1), three TMDs in parallel (TMD-3), seven TMDs in parallel (TMD-7), and two TMDs in series (STMD) are obtained. Results are reported in the following figures. In Figure 8, the maximum stress oscillation without TMD is illustrated (2 locomotives and first 8 coaches); analytical results are compared with that of the finite element (FE) solution obtained with the MIDAS Civil software. In FE modelling, the TMDs are modelled as damper unit, with elastic bilinear dapshot: results obtained for these two methods agree very well with each other. In Figure 9, the comparison of the numerical dynamic analysis results for the hotspot detail with (TMD-1, TMD-3) or without TMD solutions (wTMD-FEM) is presented, while in Figure 10, the comparison of the numerical dynamic analysis results for the hotspot detail with (TMD-7, STMD) or without TMD solutions (wTMD-FEM) is reported. It can be observed that all TMD devices are much effective at peak-point stress oscillations, significantly reducing the structural response. In particular, TMD-3 and TMD-7 devices show a better attenuation performance than the other devices. For multiple parallel TMDs, the structural response reduces with increasing the number of absorbers, as expected [41, 60, 67]. In Figure 11, a comparison of the bridge midspan displacements in frequency domain for different TMD attachments is presented, where ω and ω_1 represent the excitation frequency and the bridge fundamental frequency, respectively.

The damage caused by the passage of a single train was calculated according to Instruction 44/F (1992) first by using the rain-flow counting method to convert the irregular stress

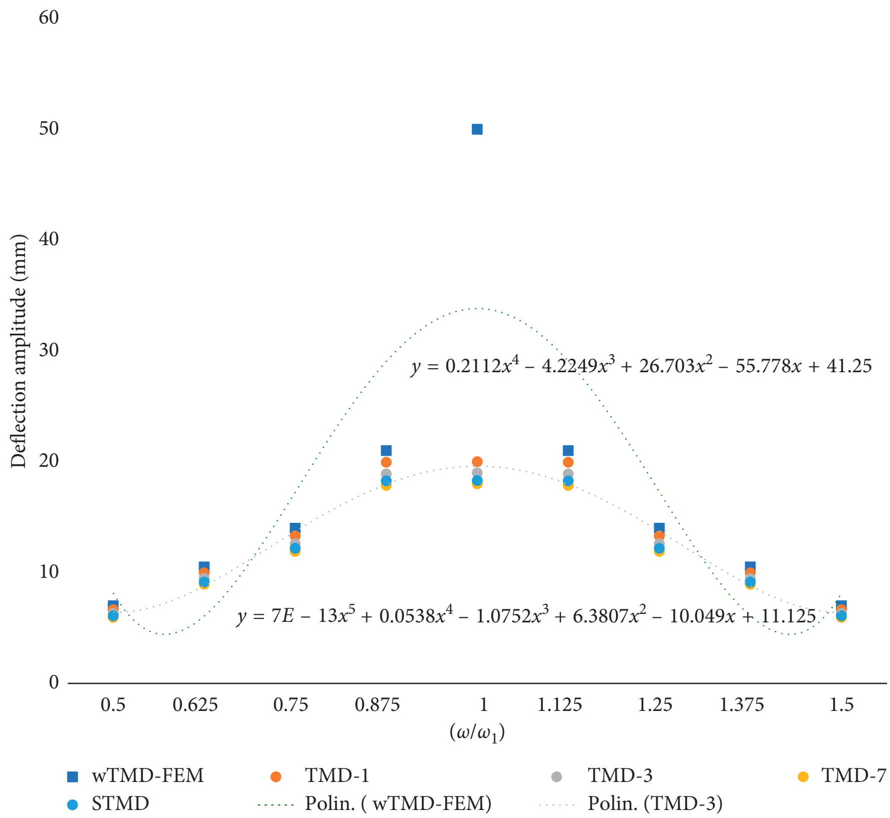

Figure 11: Variation of the deflection amplitude of the bridge at its midspan with the normalized excitation frequency for different TMD solutions.

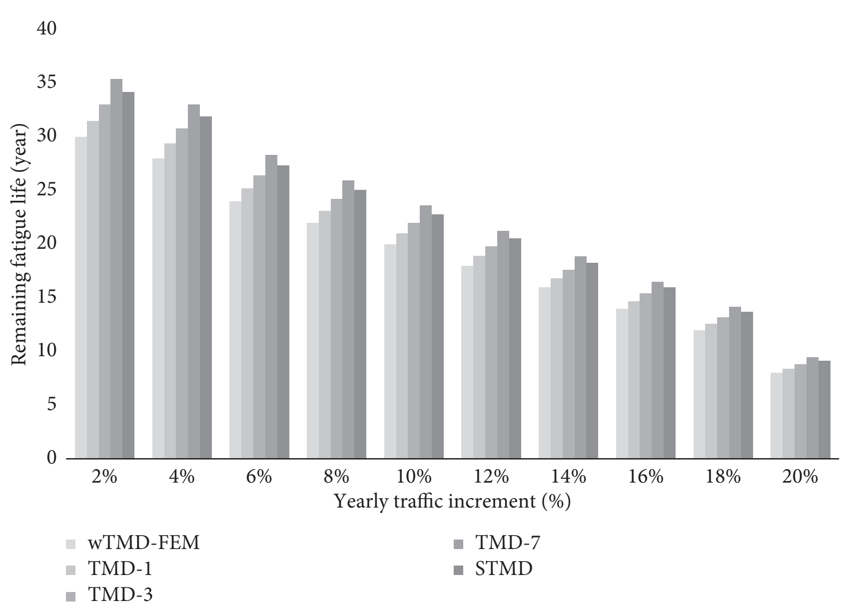

Figure 12: Yearly traffic increment (%) vs. remaining fatigue life in (year).

history into stress range blocks and then by applying the rule mentioned in [68, 69]. The cumulative damage approach implies the use of the following formula:

$$D_{d,EC_a} = \sum_{i}^{n} \frac{n_{E_i}}{N_{R_i}} \leq 1.0, \quad (20)$$

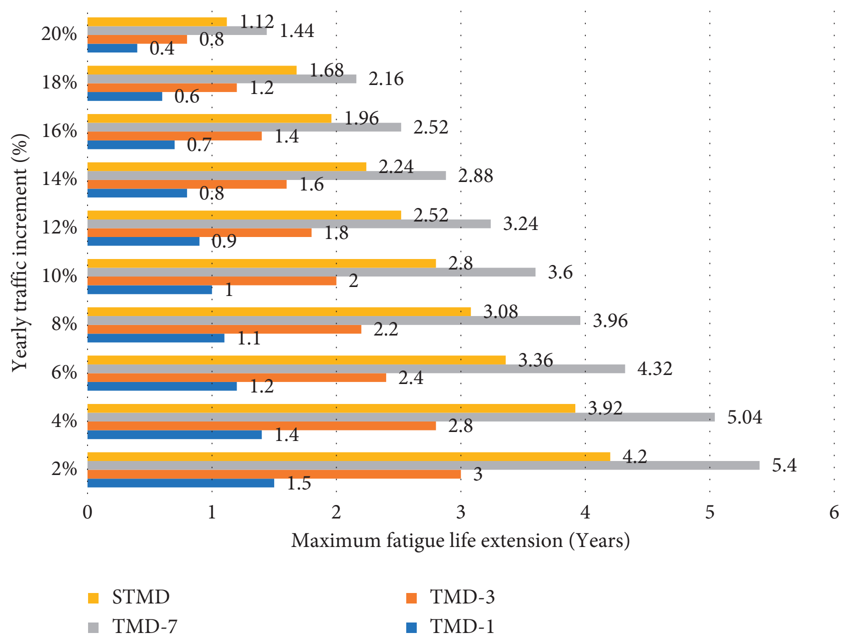

Figure 13: Maximum fatigue life extension in (year) vs. yearly traffic increment (%).

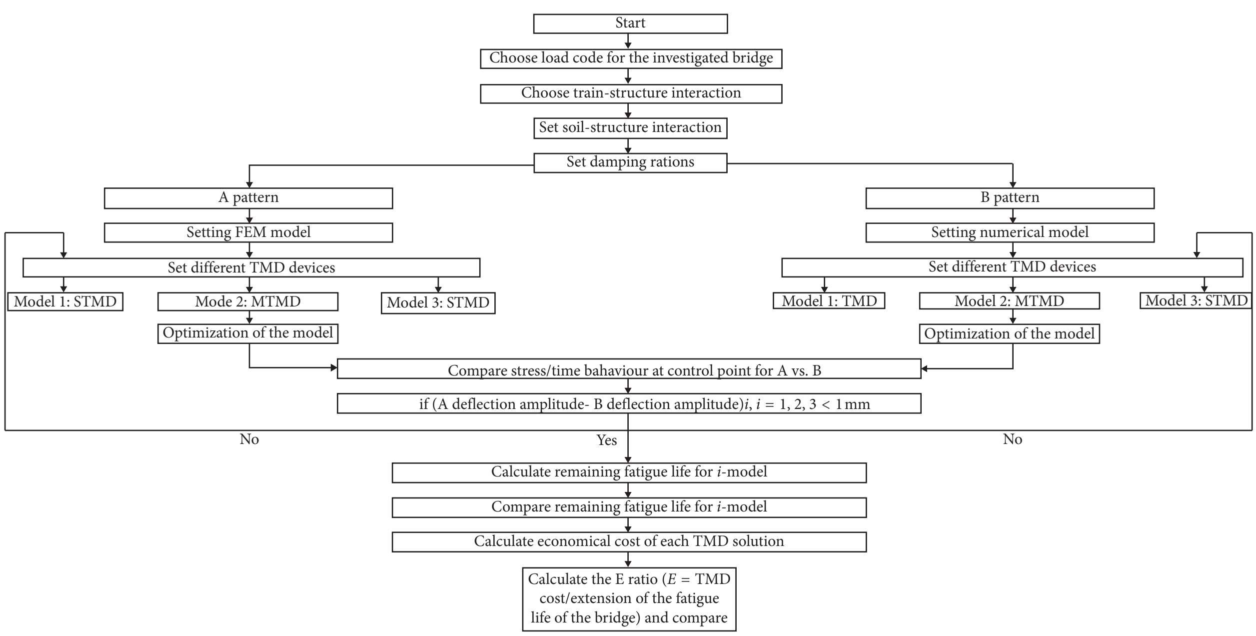

Figure 14: Flowchart of the optimization process to extend the fatigue life of steel truss bridges by tuned mass damper adoption.

where n_{E_i} is the number of cycles associated with the stress range γ_{F_f} for band "i" in the factored spectrum, (MPa); N_{R_i} is the endurance (in cycles) obtained from the factored $(\Delta\sigma_C/\gamma_{M_f})$ vs. N_R curve for a stress range of $\gamma_{F_f}\Delta\sigma_i$ (MPa), where $\Delta\sigma_C$ is the reference value of the fatigue strength at $N_C = 2$ mil cycles (MPa) and γ_{M_f} is the partial factor for fatigue strength $\Delta\sigma_C$. A precise estimation of the remaining life of the bridge, focusing on trends type of future traffic demands, with a variable increment of traffic (from 2% to 20% per year) for each train type is given; no increase in loads has been taken into account. The fatigue category of the critical detail investigated is $C = 90$, according to the Eurocode [70, 71]. According to this analysis, it should be noticed that not remarkable variation in the remaining fatigue life could be achieved by the use of TMD in existing steel railway trusses: in detail, for a yearly traffic increment of 2%, a maximum extension of the fatigue life is approximately 5 years adopting the TMD-7 solution (Figures 12 and 13). As could be inferred from Figure 13, the specific case study solved in the present paper has shown that the increase in the remaining life is at best the 15% of the actual remaining life. A final flowchart to optimize the parameters of single TMD and multiple TMD (MTMD) to extend the fatigue life of steel truss bridges is provided in Figure 14 [72–74].

9. Conclusions

In this study, the efficiency of TMD on existing steel bridges in order to extend their fatigue life is studied, elaborating an analytical formulation compared with FEM analysis. Different TMD devices (single TMD, and parallel multiple TMDs) in suppressing the maximum stress oscillation of railway bridges under railway traffic are studied. According to the results obtained, the following conclusions can be drawn: TMD-7 with seven absorbers units has the similar control effectiveness as TMD-3 with three absorbers (of different mass ratio). Therefore, the use of STMD in bridge remaining life is acceptable and similar to the capacity of multiple TMDs and may be more economical than that of multiple parallel TMDs. Considering that STMD device is robust to the main system parameters' change as much as MTMD devices and is more robust to the absorber's parameter changes than MTMD devices according to the study in [60], STMD solution is found to be the most appropriate solution to extend the fatigue life of an existing steel truss bridge. Although considering that the specific case study solved in the present paper has shown that the increase in the remaining life is at best the 15% of the actual remaining life, appropriate economic analysis is recommended, in order to compare the extension obtained in years of fatigue life of the bridge and the investment required to install the correct TMD solution, which should be studied for every particular situation.

Data Availability

The main data that support the findings of this study are available from http://www.alessiopipinato.it/publications.htm.

Conflicts of Interest

The author declares that there are no conflicts of interest.

References

[1] ASCE, "Committee on fatigue and fracture reliability of the committee on structural safety and reliability of the structural division. Fatigue reliability: parts 1–4," *Journal of the Structural Division*, vol. 108, no. ST1, pp. 3–88, 1982.

[2] J. W. Fisher, *Fatigue and Fracture of Steel Bridges: Case Studies*, Willey-Interscience, Hoboken, NJ, USA, 1984.

[3] B. Hansen, "Sensing 'Skin' may detect bridge cracks," *Civil Engineering Magazine Archive*, vol. 77, no. 10, pp. 12–14, 2007.

[4] B. Akesson and B. Edlund, "Remaining fatigue life of riveted railway bridges: Akesson, B. and Edlund B. Stahlbau (1996) 65(11), 429–436," *International Journal of Fatigue*, vol. 20, no. 1, 75 pages, 1998.

[5] P. Albrecht and A. Lenwari, "Design of prestressing tendons for strengthening steel truss bridges," *Journal of Bridge Engineering*, vol. 13, no. 5, pp. 449–454, 2008.

[6] P. Albrecht and A. Lenwari, "Variable-amplitude fatigue strength of structural steel bridge details: review and simplified model," *Journal of Bridge Engineering*, vol. 14, no. 4, pp. 226–237, 2009.

[7] M. I. Boulent, T. Righiniotis, and M. K. Chryssanthopoulos, "Probabilistic fatigue evaluation of riveted railway bridges," *ASCE Journal of Bridge Engineering*, vol. 13, no. 3, pp. 237–244, 2008.

[8] E. Brühwiler, I. F. C. Smith, and M. A. Hirt, "Fatigue and fracture of riveted bridge members," *Journal of Structural Engineering*, vol. 116, no. 1, pp. 198–214, 1990.

[9] O. S. Bursi, F. Ferrario, and V. Fontanari, "Non-linear analysis of the low-cycle fracture behaviour of isolated Tee stub connections," *Computers & Structures*, vol. 80, no. 27-30, pp. 2333–2360, 2002.

[10] J. D. Di Battista, D. E. Adamson, and G. L. Kulak, "Fatigue strength of riveted connections," *ASCE Journal of Structural Engineering*, vol. 124, no. 7, pp. 792–797, 1997.

[11] G. L. Kulak, "Discussion of "fatigue strength of riveted bridge members" by John W. Fisher, ben T. Yen, and dayi Wang (November 1990, vol. 116, no. 11)," *Journal of Structural Engineering*, vol. 118, no. 8, pp. 2280-2281, 1992.

[12] E. B. Matar and R. Greiner, "Fatigue tests for a riveted steel railway bridge in Salzburg," *Structural Engineering International*, vol. 16, no. 3, pp. 252–260, 2006.

[13] A. Pipinato, *High-cycle fatigue behavior of historical metal riveted railway bridges*, Ph.D. thesis, University of Padova, Italy, 2008.

[14] A. Pipinato, M. Molinari, C. Pellegrino, O. S. Bursi, and C. Modena, "Fatigue tests on riveted steel elements taken from a railway bridge," *Structure and Infrastructure Engineering*, vol. 7, no. 12, pp. 907–920, 2011.

[15] A. Pipinato, C. Pellegrino, O. S. Bursi, and C. Modena, "High-cycle fatigue behavior of riveted connections for railway metal bridges," *Journal of Constructional Steel Research*, vol. 65, no. 12, pp. 2167–2175, 2009.

[16] W. G. Byers, M. J. Marley, J. Mohammadi, R. J. Nielsen, and S. Sarkani, "Fatigue Reliability Reassessment applications: state of the art paper," *Journal of Structural Engineering*, vol. 123, no. 3, pp. 277–285, 2009.

[17] A. Pipinato, "Extending the lifetime of steel truss bridges by cost-efficient strengthening interventions," *Structure and Infrastructure Engineering*, vol. 14, no. 12, pp. 1611–1627, 2018.

[18] EN 1993-1-1, *Eurocode 3: Design of Steel Structures–Part 1.1: General Rules*, CEN-European Committee for Standardization, Brussels, Belgium, 2005.

[19] E. Ghafoori and M. Motavalli, "Innovative CFRP-prestressing system for strengthening metallic structures," *Journal of Composites for Construction*, vol. 19, no. 6, article 04015006, 2015.

[20] A. Pipinato, R. Pavan, P. Collin et al., "Steel bridge structural retrofit: innovative and light-weight solutions," in *Proceedings of the IALCCE 2018-The Sixth International Symposium on Life-Cycle Civil Engineering*, Taylor & Francis Group, Ghent, Belgium, ISBN 978-1-138-62633-1, Ghent, Belgium, October 2018.

[21] E. O. Ayorinde and G. B. Warburton, "Minimizing structural vibrations with absorbers," *Earthquake Engineering & Structural Dynamics*, vol. 8, no. 3, pp. 219–236, 1980.

[22] L. Cao and C. Li, "Tuned tandem mass dampers-inerters with broadband high effectiveness for structures under white noise base excitations," *Structural Control and Health Monitoring*, vol. 26, no. 4, article e2319, 2019.

[23] Y. Chen and D. S. Chen, "Timoshenko beam with tuned mass dampers to moving loads," *Journal of Bridge Engineering*, vol. 9, no. 2, 2004.

[24] J. P. Den Hartog, *Mechanical Vibrations*, McGraw-Hill, New York, NY, USA, 4th edition, 1962.

[25] R. G. Jacquot, "Optimal dynamic vibration absorbers for general beam systems," *Journal of Sound and Vibration*, vol. 60, no. 4, pp. 535–542, 1978.

[26] R. G. Jacquot and D. L. Hoppe, "Optimal random vibration absorbers," *Journal of the Engineering Mechanics Division*, vol. 99-3, pp. 612–616, 1973.

[27] M. Klasztorny, "Reduction of steady-state forced vibrations of structures with dynamic absorbers," *Earthquake Engineering & Structural Dynamics*, vol. 24, no. 8, pp. 1155–1172, 1995.

[28] B. G. Korenev and L. M. Reznikov, *Dynamic Vibration Absorbers: Theory and Technical Applications*, Wiley, New York, NY, USA, 1983.

[29] M. Abé and Y. Fujino, "Dynamic characterization of multiple tuned mass dampers and some design formulas," *Earthquake Engineering & Structural Dynamics*, vol. 23, no. 8, pp. 813–835, 1994.

[30] S. E. Randal, D. M. Halsted, and D. L. Taylor, "Optimal vibration absorbers for linear damped system," *Journal of Mechanical Design*, vol. 103, no. 4, pp. 908–913, 1981.

[31] J. C. Snowdon, *Vibration and Shock in Damped Mechanical System*, Wiley, New York, NY, USA, 1968.

[32] J. C. Snowdon, "Vibration of simply supported rectangular and square plates to which lumped masses and dynamic vibration absorbers are attached," *Journal of the Acoustical Society of America*, vol. 57, no. 3, pp. 646–654, 1975.

[33] A. Soom and M.-s. Lee, "Optimal design of linear and nonlinear vibration absorbers for damped systems," *Journal of Vibration Acoustics Stress and Reliability in Design*, vol. 105, no. 1, pp. 112–119, 1983.

[34] G. B. Warburton, "Reduction of harmonic response of cylindrical Shells," *Journal of Engineering for Industry*, vol. 97, no. 4, pp. 1371–1377, 1975.

[35] G. B. Warburton, "Optimum absorber parameters for minimizing vibration response," *Earthquake Engineering & Structural Dynamics*, vol. 9, no. 3, pp. 251–262, 1981.

[36] G. B. Warburton, "Optimum absorber parameters for various combinations of response and excitation parameters," *Earthquake Engineering & Structural Dynamics*, vol. 10, no. 3, pp. 381–401, 1982.

[37] H.-C. Kwon, M.-C. Kim, and I.-W. Lee, "Vibration control of bridges under moving loads," *Computers & Structures*, vol. 66, no. 4, pp. 473–480, 1998.

[38] C. C. Lin, J. F. Wang, and B. L. Chen, "Train-induced vibration control of high-speed railway bridges equipped with multiple tuned mass dampers," *Journal of Bridge Engineering*, vol. 10, p. 4, 2005.

[39] J.-D. Yau and Y.-B. Yang, "A wideband MTMD system for reducing the dynamic response of continuous truss bridges to moving train loads," *Engineering Structures*, vol. 26, no. 12, pp. 1795–1807, 2004.

[40] M. Gu, S. R. Chen, and C. C. Chang, "Parametric study on multiple tuned mass dampers for buffeting control of Yangpu Bridge," *Journal of Wind Engineering and Industrial Aerodynamics*, vol. 89, no. 11-12, pp. 987–1000, 2001.

[41] C. Li, "Design parameters multiple tuned mass dampers for attenuating torsional vibration of one-storey asymmetric structures," *Journal of Vibration and Shock*, vol. 24, no. 1, pp. 118–120, 2005.

[42] Z. Chen, Z. Han, W. Zhai, and J. Yang, "TMD design for seismic vibration control of high-pier bridges in Sichuan–Tibet Railway and its influence on running trains," *International Journal of Vehicle Mechanics and Mobility*, vol. 57, pp. 207–225, 2019.

[43] A. Chopra, *Dynamics of Structures*, Pearson Edition, New York, NY, USA, 2004.

[44] L. Frýba, "A rough assessment of railway bridges for high speed trains," *Engineering Structures*, vol. 23, no. 5, pp. 548–556, 2001.

[45] J. L. Humar, *Dynamics of Structures*, CRC Press, Boca Raton, FL, USA, 2012.

[46] Karoumi, *Response of cable-stayed and suspension bridges to moving vehicles*, Ph.D. thesis, Royal Institute of Technology-KTH, TRITA-BKN, 1998.

[47] S. S. Rao, *Vibration of Continuous Systems*, John Wiley & Sons, Inc, Hoboken, NJ, USA, 2007, ISBN-13 978-0-471-77171-5.

[48] H. Saller, *Einfluss bewegter Last auf Eisenbahnoberbau und Brücken*, Kreidels, Berlin, Germany, 1921.

[49] K. Liu, G. De Roeck, and G. Lombaert, "The effect of dynamic train-bridge interaction on the bridge response during a train passage," *Journal of Sound and Vibration*, vol. 325, no. 1-2, pp. 240–251, 2009.

[50] CEN, *EN 1991:2: Eurocode 1: Actions on Structures–Part 2: Traffic Loads on Bridges*, CEN, Brussels, Belgium, 2003.

[51] A. Romero, M. Solís, and P. Galvín, "Soil-structure interaction in resonant railway bridges," *Soil Dynamics and Earthquake Engineering*, vol. 47, pp. 108–116, 2013.

[52] A. Tosecky, *Wave propagation in homogeneous elastic half-space using the dual reciprocity boundary element method*, Ph.D. thesis, Dissertation at the Faculty of Civil Engineering, Ruhr University Bochum, Bochum, Germany, 2005.

[53] M. Ülker-Kaustell and R. Karoumi, "Influence of non-linear stiffness and damping on the train-bridge resonance of a simply supported railway bridge," *Engineering Structures*, vol. 41, pp. 350–355, 2012.

[54] M. Ülker-Kaustell, R. Karoumi, and C. Pacoste, "Simplified analysis of the dynamic soil-structure interaction of a portal frame railway bridge," *Engineering Structures*, vol. 32, no. 11, pp. 3692–3698, 2010.

[55] Y. B. Yang and J. D. Yau, "An iterative interacting method for dynamic analysis of the maglev train-guideway/foundation-soil system," *Engineering Structures*, vol. 33, no. 3, pp. 1013–1024, 2011.

[56] ERRI D-214, *Rail Bridges for Speeds Over 200 km/h, Recommendations for Calculating Damping in Rail Bridge Decks*, 1999.

[57] S. A. Neild, *Using non-linear vibration techniques to detect damage in concrete bridges*, Ph.D. thesis, University of Oxford, Oxford, UK, 2001.

[58] A. Pipinato, C. Pellegrino, and C. Modena, "Assessment procedure and rehabilitation criteria for the riveted railway Adige Bridge," *Structure and Infrastructure Engineering*, vol. 8, no. 8, pp. 747–764, 2012.

[59] CEN, *EN 10025-1:2004–European Standard for Hot-Rolled Structural Steel*, CEN, Brussels, Belgium, 2004.

[60] V. Kahya and O. Araz, "Series tuned mass dampers in train-induced vibration control of railway bridges," *Structural Engineering and Mechanics*, vol. 61, no. 4, pp. 453–461, 2017.

[61] A. Brencich and L. Gambarotta, "Assessment procedure and rehabilitation of riveted railway girders: the Campasso Bridge," *Engineering Structures*, vol. 31, no. 1, pp. 224–239, 2009.

[62] C. Li and B. Zhu, "Estimating double tuned mass dampers for structures under ground acceleration using a novel optimum

criterion," *Journal of Sound and Vibration*, vol. 298, no. 1-2, pp. 280–297, 2006.

[63] Y. Yang and J. Yau, *Vehicle-bridge Interaction Dynamics, with Application to High-Speed Railways*, World Scientific, Singapore, 2004.

[64] L. Zuo, "Effective and robust vibration control using series multiple tuned-mass dampers," *Journal of Vibration and Acoustics*, vol. 131, no. 3, article 031003, 2009.

[65] K. Xu and T. Igusa, "Dynamic characteristics of multiple substructures with closely spaced frequencies," *Earthquake Engineering & Structural Dynamics*, vol. 21, no. 12, pp. 1059–1070, 1992.

[66] T. Bandivadekar and R. Jangid, "Optimization of multiple tuned mass dampers for vibration control of system under external excitation," *Journal of Vibration and Control*, vol. 19, no. 12, pp. 1854–1871, 2012.

[67] M. Luu, V. Zabel, and C. Könke, "An optimization method of multi-resonant response of high-speed train bridges using TMDs," *Finite Elements in Analysis and Design*, vol. 53, pp. 13–23, 2012.

[68] M. A. Miner, "Cumulative damage in fatigue," *Journal of Applied Mechanics*, vol. 12, pp. A159–A164, 1945.

[69] A. G. Palmgren, "Die lebensdauer von Kugellagern (life length of roller bearings or durability of ball bearings)," *Zeitschrift des Vereines Deutscher Ingenieure (ZVDI)*, vol. 14, pp. 339–341, 1924.

[70] EN 1993-1-9, *Eurocode 3: Design of Steel Structures–Part 1-9: Fatigue*, CEN, Brussels, Belgium, 2005.

[71] A. Pipinato, C. Pellegrino, and C. Modena, "Residual life of historic riveted steel bridges: an analytical approach," *Proceedings of the Institution of Civil Engineers-Bridge Engineering*, vol. 167, no. 1, pp. 17–32, 2014.

[72] G. B. Warburton and E. O. Ayorinde, "Optimum absorber parameters for simple systems," *Earthquake Engineering & Structural Dynamics*, vol. 8, no. 3, pp. 197–217, 1980.

[73] Y. B. Yang and C. W. Lin, "Vehicle-bridge interaction dynamics and potential applications," *Journal of Sound and Vibration*, vol. 284, no. 1-2, pp. 205–226, 2005.

[74] J. D. Yau and Y. B. Yang, "Vibration reduction for cable-stayed bridges traveled by high-speed trains," *Finite Elements in Analysis and Design*, vol. 40, no. 3, pp. 341–359, 2004.


Journal of Engineering
The Scientific World Journal
International Journal of Rotating Machinery
Journal of Sensors
Advances in Multimedia
Advances in Civil Engineering
Hindawi
Submit your manuscripts at
www.hindawi.com
Journal of Control Science and Engineering
Journal of Robotics
Journal of Electrical and Computer Engineering
Advances in OptoElectronics
VLSI Design
International Journal of Navigation and Observation
Modelling & Simulation in Engineering
International Journal of Aerospace Engineering
International Journal of Chemical Engineering
International Journal of Antennas and Propagation
Active and Passive Electronic Components
Shock and Vibration
Advances in Acoustics and Vibration